

Post-Periastron Gamma Ray Flare from PSR B1259–63/LS 2883 as a Result of Comptonization of the Cold Pulsar Wind

Dmitry Khangulyan¹, Felix A. Aharonian^{2,3}, Sergey V. Bogovalov⁴, Marc Ribó⁵

¹*Institute of Space and Astronautical Science/JAXA, 3-1-1 Yoshinodai, Chuo-ku, Sagamihara, Kanagawa 252-5210, Japan*

khangul@astro.isas.jaxa.jp

²*Dublin Institute for Advanced Studies, 31 Fitzwilliam Place, Dublin 2, Ireland*

felix.aharonian@dias.ie

³*Max-Planck-Institut für Kernphysik, Saupfercheckweg 1, D-69117 Heidelberg, Germany*

⁴*National Research Nuclear University (MEPHI), Kashirskoe shosse 31, Moscow, 115409 Russia*

svbogovalov@mephi.ru

⁵*Departament d’Astronomia i Meteorologia, Institut de Ciències del Cosmos (ICC), Universitat de Barcelona (IEEC-UB), Martí i Franquès 1, E-08028 Barcelona, Spain*

mribo@am.ub.es

ABSTRACT

We argue that the bright flare of the binary pulsar PSR B1259–63/LS2883 detected by the *Fermi* Large Area Telescope (LAT), is due to the inverse Compton (IC) scattering of the unshocked electron-positron pulsar wind with a Lorentz factor $\Gamma_0 \approx 10^4$. The combination of two effects both linked to the circumstellar disk (CD), is a key element in the proposed model. The first effect is related to the impact of the surrounding medium on the termination of the pulsar wind. Inside the disk, the “early” termination of the wind results in suppression of its gamma-ray luminosity. When the pulsar escapes the disk, the conditions for termination of the wind undergo significant changes. This would lead to a dramatic increase of the pulsar wind zone, and thus to the proportional increase of the gamma-ray flux. On the other hand, if the parts of the CD disturbed by the pulsar can supply infrared photons of density high enough for efficient Comptonization of the wind, almost the entire kinetic energy of the pulsar wind

would be converted to radiation, thus the gamma-ray luminosity of the wind could approach to the level of the pulsar’s spin-down luminosity as reported by the *Fermi* collaboration.

Subject headings: binaries: close — gamma rays: stars — radiation mechanisms: non-thermal — pulsars: individual (PSR B1259–63) — stars: individual (LS2883)

1. Introduction

The pulsar magnetospheres are effective gamma-ray emitters (Abdo et al. 2010). Pulsars can produce potentially detectable gamma-ray emission also due to the bulk Comptonization of their cold ultrarelativistic winds. While in the case of isolated pulsars this radiation component is generally weak, unless the wind is accelerated (relatively) close to the pulsar (Bogovalov & Aharonian 2000; Aharonian et al. 2012), in binary systems the radiation is significantly enhanced due to the presence of dense target photon field supplied by the optical companion (Ball & Kirk 2000; Ball & Dodd 2001; Khangulyan et al. 2007, 2011). Gamma-rays are produced also after termination of the wind due to the IC scattering of relativistic electrons accelerated by the termination shock. In isolated pulsars the termination of the wind leads to the formation of the so-called Pulsar Wind Nebulae with a distinct extended synchrotron and IC emission which can be easily separated from the radiation of the unshocked wind. In binary pulsars, the separation of the radiation components produced before and after the termination of the pulsar wind is a more difficult task; it requires careful analysis of the spectral and temporal features of two radiation components.

The most promising object for exploration of processes of formation, acceleration and termination of pulsar winds in binary systems is PSR B1259–63/LS2883. It contains a 47.7 ms pulsar orbiting a luminous star in a very eccentric orbit (eccentricity $e = 0.87$, period $P_{\text{orb}} = 1237$ d, semi-major axis $a_2 = 7.2$ AU, see Johnston et al. 1992; Negueruela et al. 2011, and references therein). The variable TeV gamma-ray emission detected from this object by the H.E.S.S. collaboration (Aharonian et al. 2005, 2009) was in general agreement with the predictions (Kirk et al. 1999), but the TeV gamma-ray lightcurve appeared to be different from expectations. Several possible scenarios suggested for interpretation of the reported TeV lightcurve (Khangulyan et al. 2007), predict essentially different gamma-ray fluxes at MeV/GeV energies, therefore the measurements in this energy band should significantly contribute to the understanding of the hydrodynamics and the particle acceleration processes in binary pulsars.

The recent observations of PSR B1259–63/LS2883 with *Fermi* LAT revealed a complex behavior of the system in GeV gamma-rays (Abdo et al. 2011; Tam et al. 2011). Close to the periastron passage, the source has been detected with a modest energy flux of $6 \times 10^{-11} \text{erg cm}^{-2} \text{s}^{-1}$. However, +30 days after periastron passage (with largest recorded flux level at +35 days), a spectacular flare has been recorded. It lasted approximately two weeks with an enhanced flux above 100 MeV at the level of $3 \times 10^{-10} \text{erg cm}^{-2} \text{s}^{-1}$ (Abdo et al. 2011; Tam et al. 2011). The flare is characterized by a sharp increase and a rather smooth decay over approximately 2 weeks. Importantly, the strong increase of gamma ray flux was not accompanied by a noticeable change of the X-ray flux (Abdo et al. 2011). While the weak GeV flux reported during the periastron passage can be explained by IC scattering of electrons accelerated at the termination shock and/or by the bulk Comptonization of the unshocked electron-positron wind (Khangulyan et al. 2011), the post-periastron flare was a real surprise. In general, this flare represents a unique case in astrophysics when the available energy of an object is fully converted to nonthermal high energy radiation. On the other hand, given the current belief that the rotational energy of the pulsar is converted to kinetic energy of cold ultrarelativistic electron-positron wind, the binary pulsars can in principle operate as perfect ‘100 %’ efficient gamma-ray emitters if the density of the surrounding target photon field would be high enough for realization of Comptonization of the pulsar wind in the saturation regime. Yet, any explanation of this flare should address several important issues, namely (i) the extraordinary high luminosity of gamma radiation at the level close to the pulsar’s spin-down luminosity (SDL), $\dot{E} = 8 \times 10^{35} \text{erg/s}$; (ii) lack of enhanced non-thermal X-ray flux; (iii) orbital phase of the flare.

2. The scenario

The very fact of absence of simultaneous activity in the X-ray energy band suggests that the gamma-ray emission is produced by the pulsar wind. Indeed, since in the cold wind the electrons move together with magnetic field, they lose their energy only through the IC scattering, thus IC gamma-rays are emitted without accompanying synchrotron radiation. Moreover, for a narrow, e.g. Planckian type distribution of ambient photons with temperature T_r , the upscattered gamma-ray emission will be concentrated within a narrow energy interval with a characteristic energy $E_\gamma \approx 3kT_r\Gamma_0^2 \approx 300(kT_r/1 \text{ eV})\Gamma_{0,4}^2 \text{ MeV}$ in the Thomson regime ($kT_r\Gamma_0/m_e^2c^4 \ll 1$) or $E_\gamma \approx m_e c^2 \Gamma_0 \approx 5\Gamma_{0,4} \text{ GeV}$ in the Klein-Nishina regime ($kT_r\Gamma_0/m_e^2c^4 \geq 1$). Here $\Gamma_0 = 10^4\Gamma_{0,4}$ is wind bulk Lorentz factor.

The strength of the gamma-ray signal produced by the wind depends on three parameters: (i) the bulk Lorentz factor of the wind, (ii) the density of the target photon

field, (iii) the pulsar wind zone (PWZ) length towards the observer (see e.g. Ball & Dodd 2001; Khangulyan et al. 2007; Sierpowska-Bartosik & Bednarek 2008; Cerutti et al. 2008; Khangulyan et al. 2011). At least one of these parameters should experience sudden changes in order to provide a sharp increase of the gamma-ray signal as detected by *Fermi* LAT. Bogovalov et al. (2008) have shown that the interaction of the pulsar wind can proceed in two different regimes depending on the ratio η of ram pressures of the interacting pulsar and stellar winds. For $\eta < \eta_{\text{cr}}$, where $\eta_{\text{cr}} \simeq 10^{-2}$, the pulsar wind termination shock has a closed structure, and for $\eta > \eta_{\text{cr}}$ the termination shock is expected to be unclosed (on a scale of the binary system, see Bosch-Ramon & Barkov 2011; Bosch-Ramon et al. 2012). This hydrodynamical instability should lead to a fast (on timescales of $10^3 - 10^4$ s) transformation of the termination shock. Importantly, in the case of interaction of the pulsar with the CD $\eta_{\text{d}} \sim 10^{-3} \ll \eta_{\text{cr}}$, while at the interaction of the pulsar wind with the stellar wind (SW) $\eta_{\text{w}} \sim 5 \times 10^{-2} \gg \eta_{\text{cr}}$ (Khangulyan et al. 2011). Thus, the pulsar’s entrance to and exit from the CD should lead to fast transformations of the termination shock. In Figure 1, we show PWZ lengths calculated for different orbital inclinations and the η parameter (for details see Khangulyan et al. 2011).

The increase of the PWZ length by a factor of ~ 10 after its escape of the disk naturally explains the detected dramatic increase of the gamma-ray flux during the flare (see Fig. 2). What concerns the absolute gamma-ray flux with corresponding luminosity comparable to the pulsar’s SDL, it requires that the Comptonization of the wind electrons proceeds in the optically thick regime, i.e. the IC cooling length l_{IC} should not exceed the PWZ length of about $l_{\text{IC}} \sim 10^{13}$ cm outside the disk. In the Thomson regime,

$$l_{\text{IC}} \simeq 10^{14} \Gamma_{0,4}^{-1} (w_{\text{ph}} / \text{erg cm}^{-3})^{-1} \text{cm}, \quad (1)$$

where w_{ph} is target photons energy density. Thus, the required energy density of the target photon field is

$$w_{\text{ph}} \simeq 10 \Gamma_{0,4}^{-1} l_{\text{IC},13}^{-1} \text{erg cm}^{-3}, \quad (2)$$

where $l_{\text{IC},13} = l_{\text{IC}} / (10^{13} \text{cm})$. Although the luminosity of the optical companion LS 2883 is rather high (Negueruela et al. 2011), it is still not sufficient for realization of the optically thick IC scenario (Khangulyan et al. 2011). The CD is another source of target photons for Compton scattering of electrons (van Soelen & Meintjes 2011), which contribution can be significant (especially in the close vicinity of the disk). Equations (1) and (2) give an estimate of the required luminosity of the target photon field

$$L_{\text{ph}} > 10^{38} \Gamma_{0,4}^{-1} l_{\text{IC},13} \text{erg s}^{-1}. \quad (3)$$

This is a quite tough requirement, as large as 40 % of the luminosity of the optical companion (Negueruela et al. 2011). One may speculate that such a high photon field is a result of

thermal radiation of the heated parts of the CD triggered e.g. by the interaction of the pulsar with the disk. Whether such an effective heating of the disk is possible is an open issue. While the answer to this question requires detailed hydrodynamical studies, below we simply postulate the existence of such a high density radiation field.

The requirement on the luminosity of the target photon field given by Eq. (3), can be relaxed assuming larger wind bulk Lorentz factors and/or smaller values of l_{IC} . The Lorentz factor cannot much exceed 10^4 , unless the temperature of radiation is significantly less than 10^4K (to explain the reported energy spectrum of gamma-rays). However, for $T_r \ll 10^4\text{K}$, the required energy density of the photon field would exceed the Stefan-Boltzmann limit for black-body radiation. Regarding the size of the region filled with photon field, it cannot be smaller than $> 10^{13}\text{cm}$, given that during the flare (from +30d to +60d from periastron passage) the star separation distance changes from $3.7 \times 10^{13}\text{cm}$ to $6 \times 10^{13}\text{cm}$.

In the framework of the proposed model, one should expect a similar flare when the pulsar exits the disk during the pre-periastron epoch. However, due to the differences in the termination shock orientation, the intensity of this flare should be different (see Fig.3). Assuming that the pulsar exits the disk at epochs symmetric in terms of true anomaly, the pre-periastron exit should occur 10 days before the periastron passage. For $\eta = 5 \times 10^{-2}$ the ratio of PWZ lengths corresponding to +30 d and -10 d epochs exceeds 4 (see Figs. 1 and 2), therefore the expected flux level is consistent with the *Fermi* LAT upper limits obtained for that period.

Below we present and discuss the results of numerical calculations performed within the suggested scenario. The formalism applied to PSR B1259–63/LS2883 is described in our previous papers (Khangulyan et al. 2007, 2011). The calculations rely on hydrodynamical simulations of interaction of the pulsar and CD (Bogovalov et al. 2008, 2012). In this paper we include the effects related to the presence of the CD which have not been taken into account in previous studies.

3. Radiation of the unshocked pulsar wind

In Figure 4 we show the spectral energy distribution (SED) of IC radiation of the pulsar wind averaged over the period of *Fermi* LAT observations (Abdo et al. 2011). The calculations are performed for different values of the initial Lorentz factor Γ_0 and the η - parameter. These value correspond to the following regimes: $\eta = 1$ – upper limit; $\eta = 0.05$ – interaction with the SW; $\eta = 10^{-3}$ – interaction with the CD (see Khangulyan et al. 2011, for details). The comparison of calculations with the *Fermi* data shows that the IC

radiation of the unshocked wind can achieve the level of reported fluxes. However, these fluxes are also rather close to theoretical predictions for radiation of the shocked wind (see Figs. 7 and 13 in Khangulyan et al. 2007). Unfortunately the marginal gamma-ray signal obtained during the periastron passage does not allow a quantitative analysis which would give preference to the radiation associated with the wind before or after its termination. On the other hand, the detected gamma-ray fluxes can be treated as upper limits for the unshocked wind component. This allow us to constrain the wind’s Lorentz factor Γ_0 ; as it follows from Figure 4, the interval of $\Gamma_0 \sim (0.1 - 3) \times 10^5$ is excluded by the gamma-ray data.

The gamma-ray signal from the pulsar wind associated with the target photons of the companion star has a smooth orbital phase dependence (Khangulyan et al. 2011). In contrast, the CD can introduce quite sharp temporal features. Presently, the properties of CDs in binary pulsars are a subject of debate (see e.g. Okazaki et al. 2011). Here we assume that a CD does exist in PSR B1259–63/LS2883, and that it extends to 3×10^{13} cm from the star, as it follows from the eclipse of the pulsed radio emission observed in 2010 between –16 and +15 days around the periastron (Abdo et al. 2011). The impact of the disk has been taken into account by introducing two effects: (i) the change of the η -parameter; and (ii) the presence of an additional target photon field from the disk itself.

To illustrate the importance of these effects, we performed calculations corresponding to the three important cases:(a) suppression of the PWZ length by the disk, i.e. $\eta = 10^{-3}$, $t = +35$ days after periastron passage; (b) flare epoch, i.e. $\eta = 0.05$, $t = +35$; and (c) pre-periastron flare, i.e. $\eta = 0.05$, $t = -10$ days before periastron passage. The additional target photon field was assumed to be gray body with temperature $T_r = 10^4$ K and energy density $w_{\text{ph}} = 2.8 \text{ erg cm}^{-3}$. The results of calculations are shown in Fig. 2. The sudden increase of the gamma-ray flux by an order of magnitude during the flare is due to the increase of PWZ length just after the pulsar leaves the disk. During the first 1-2 weeks of this epoch the pulsar is located close to the disk, and therefore the wind zone is intensively illuminated by the photons of the disk. Apparently, the dominance of the infrared component of the disk over the optical radiation of the star, and the upper limit on the Lorentz factor of the wind derived from *Fermi* LAT observations during the periastron passage, explain quite naturally the significantly softer spectrum of gamma rays observed during the flare (Abdo et al. 2011; Tam et al. 2011). From Fig. 2 one can see that with the assumed set of three model parameters η , T_r , and Γ_0 , one can explain both the spectral shape and the absolute flux of gamma-rays during the flare. With a slightly different choice of parameters than the ones used in Fig. 2 we can provide, in principle, a perfect fit to the observational results. However, given the uncertainties related the complex character of the interaction of the wind with the disk, the ”perfect fit” would be redundant. Instead, we would like to

emphasize the most important consequences of this interpretation. First, it implies that the Lorentz factor of the wind cannot be significantly smaller than 10^4 given that the energy of the IC photons scales as $E_\gamma \propto T_r \Gamma_0^2$. On the other hand, the Fermi LAT observations during the periastron passage constrain the wind Lorentz factor to $\Gamma_0 \leq 10^4$. Thus, if our interpretation of the flare is correct, the wind Lorentz factor should be quite close to 10^4 .

4. Discussion

In this letter we propose a model for the recent *Fermi* observations of gamma-rays from PSR B1259–63/LS 2883. We assume that gamma-rays are produced at interaction of the cold pulsar wind with external photon fields. While the Comptonization of the wind by radiation of the companion star can explain the modest gamma-ray flux detected during the periastron passage, the order of magnitude higher flux of the post-periastron flare requires an additional seed photon component. We propose that the radiation of the heated CD can play this role. The Comptonization of the pulsar wind by the CD emission proceeds in a quite specific way. Inside the disk it is suppressed because of the high ram pressure in the disk. The density of the stellar optical photons generally dominates over the density of IR photons. But in the immediate vicinity of the disk, where the IR density can be still very high, the optical depth for Compton scattering might be significantly larger than 1. This would lead to a very effective, close to 100% efficiency of transformation of the rotational energy of the pulsar to high energy gamma rays via Comptonization of the cold ultrarelativistic wind. In the suggested scenario, the departure of the pulsar wind from the disk will lead to a gradual decrease of the photon density from the disk and correspondingly to the reduction of the IC gamma-ray flux on time-scales of days.

During the exit of the pulsar from the disk at the epoch before the periastron passage, the termination shock is expected to expand towards the direction opposite to the observer, thus we should not expect strong gamma-ray signal. This agrees with the *Fermi LAT* observations. The main issue for realization of the proposed scenario is whether the pulsar-disk interaction can provide the required photon field. This is a key question which should be answered by detailed studies of interaction of the pulsar wind with the CD. This study should also address another important issue, which is related to the 15 days delay between the appearance of the pulsed radio emission and the epoch of the GeV flare.

If the proposed interpretation is correct, this would be the second case of direct measurement of a pulsar wind’s Lorentz factor. Recently, the Lorentz factor of order of 10^6 has been extracted from the observation of very high energy pulsed gamma-ray emission from the Crab Pulsar (Aharonian et al. 2012). Interestingly, the two orders of magnitude smaller

Lorentz factor of the pulsar wind in PSR B1259–63/LS 2883 compared to the Crab pulsar, is quite close the ratio of spin-down luminosities of two pulsars. If this is not just a coincidence, the linear dependence $\Gamma_0 \propto L_{SD}$ would imply a universal production rate of electron-positron pairs of order of 10^{38} e^\pm /sec, independent of the pulsar spin-down luminosity.

Finally, we should note that in principle the gamma-ray flare can be explained also by the post-shock flow. Since the flux detected by *Fermi* LAT was close to pulsar’s SDL, this interpretation requires significant Doppler boosting of radiation. Relativistic flows can be indeed formed at interactions of the pulsar and SWs (Bogovalov et al. 2008), and therefore the broad-band radiation can be affected by the Doppler boosting (Khangulyan et al. 2008; Dubus et al. 2010). The Doppler boosting should amplify also the X- and TeV gamma ray fluxes. However, the lack of any noticeable activity during the flare at other wavelengths (Abdo et al. 2011) makes this interpretation less likely. Also, one should note that the flux level of the Doppler boosted radiation can easily exceed the limit set by the pulsar’s SDL, but flares with apparent super SDL so far have not been detected. On the other hand, the detection of such events in future observations would rule out the origin of gamma-radiation related to the unshocked pulsar wind.

S.V.B. acknowledges support by Federal Targeted Program “The Scientific and Pedagogical Personnel of the Innovative Russia” in 2009-2013 (state contract N 536 on May 17, 2010) and by grant of Russian Ministry of Science and Education N 2.6310.2011. M.R. acknowledges support by the Spanish Ministerio de Ciencia e Innovación (MICINN) under grant FPA2010-22056-C06-02, as well as financial support from MICINN and European Social Funds through a *Ramón y Cajal* fellowship.

REFERENCES

- Abdo, A. A., Ackermann, M., Ajello, M., et al. 2010, *ApJS*, 187, 460
- Abdo, A. A., *Fermi* LAT Collaboration, Chernyakova, M., Neronov, A., Roberts, M., & *Fermi* Pulsar Timing Consortium, 2011, *ApJ*, 736, L11
- Aharonian, F., et al. (HESS collaboration) 2005, *A&A*, 442, 1
- Aharonian, F., et al. (HESS collaboration) 2009, *A&A*, 507, 389
- Aharonian, F., Bogovalov, S., and Khangulyan, D. 2012, *Nature*, 482, 507
- Ball, L., & Kirk, J. G. 2000, *Astropart. Phys.*, 12, 335

- Ball, L., & Dodd, J. 2001, PASA, 18, 98
- Bogovalov, S. V., & Aharonian, F. A. 2000, MNRAS, 313, 504
- Bogovalov, S. V., Khangulyan, D. V., Koldoba, A. V., Ustyugova, G. V., & Aharonian, F. A. 2008, MNRAS, 387, 63
- Bogovalov, S. V., Khangulyan, D., Koldoba, A. V., Ustyugova, G. V., & Aharonian, F. A. 2012, MNRAS, 419, 3426
- Bosch-Ramon, V., & Barkov, M. V. 2011, A&A, 535, A20
- Bosch-Ramon, V., Barkov, M. V., Khangulyan, D., & Perucho, M. 2012, arXiv:1203.5528
- Cerutti, B., Dubus, G., & Henri, G. 2008, A&A, 488, 37
- Connors, T. W., Johnston, S., Manchester, R. N., & McConnell, D. 2002, MNRAS, 336, 1201
- Dubus, G., Cerutti, B., & Henri, G. 2010, A&A, 516, A18
- Johnston, S., Manchester, R. N., Lyne, A. G., Bailes, M., Kaspi, V. M., Qiao, G., & D’Amico, N. 1992, ApJ, 387, L37
- Kennel, C.F. & Coroniti, F. V. 1984, ApJ, 283, 710
- Khangulyan, D., Hnatic, S., Aharonian, F., & Bogovalov, S. 2007, MNRAS, 380, 320
- Khangulyan, D. V., Aharonian, F. A., Bogovalov, S. V., Koldoba, A. V., & Ustyugova, G. V. 2008, International Journal of Modern Physics D, 17, 1909
- Khangulyan, D., Aharonian, F. A., Bogovalov, S. V., & Ribó, M. 2011, ApJ, 742, 98
- Kirk, J. G., Ball, L., & Skjaeraasen, O. 1999, Astropart. Phys., 10, 31
- Negueruela, I., Ribó, M., Herrero, A., Lorenzo, J., Khangulyan, D., Aharonian, F.A., ApJL, 732, L11
- Okazaki, A. T., Nagataki, S., Naito, T., Kawachi, A., Hayasaki, K., Owocki, S. P. and Takata, J. 2011, PASJ, 63, 5
- Rees, M.J. & Gunn, J.E. 1974, MNRAS, 167, 1
- Sierpowska-Bartosik, A., & Bednarek, W. 2008, MNRAS, 385, 2279

van Soelen, B., & Meintjes, P. J. 2011, MNRAS, 412, 1721

Tam, P. H. T., Huang, R. H. H., Takata, J., et al. 2011, ApJ, 736, L10

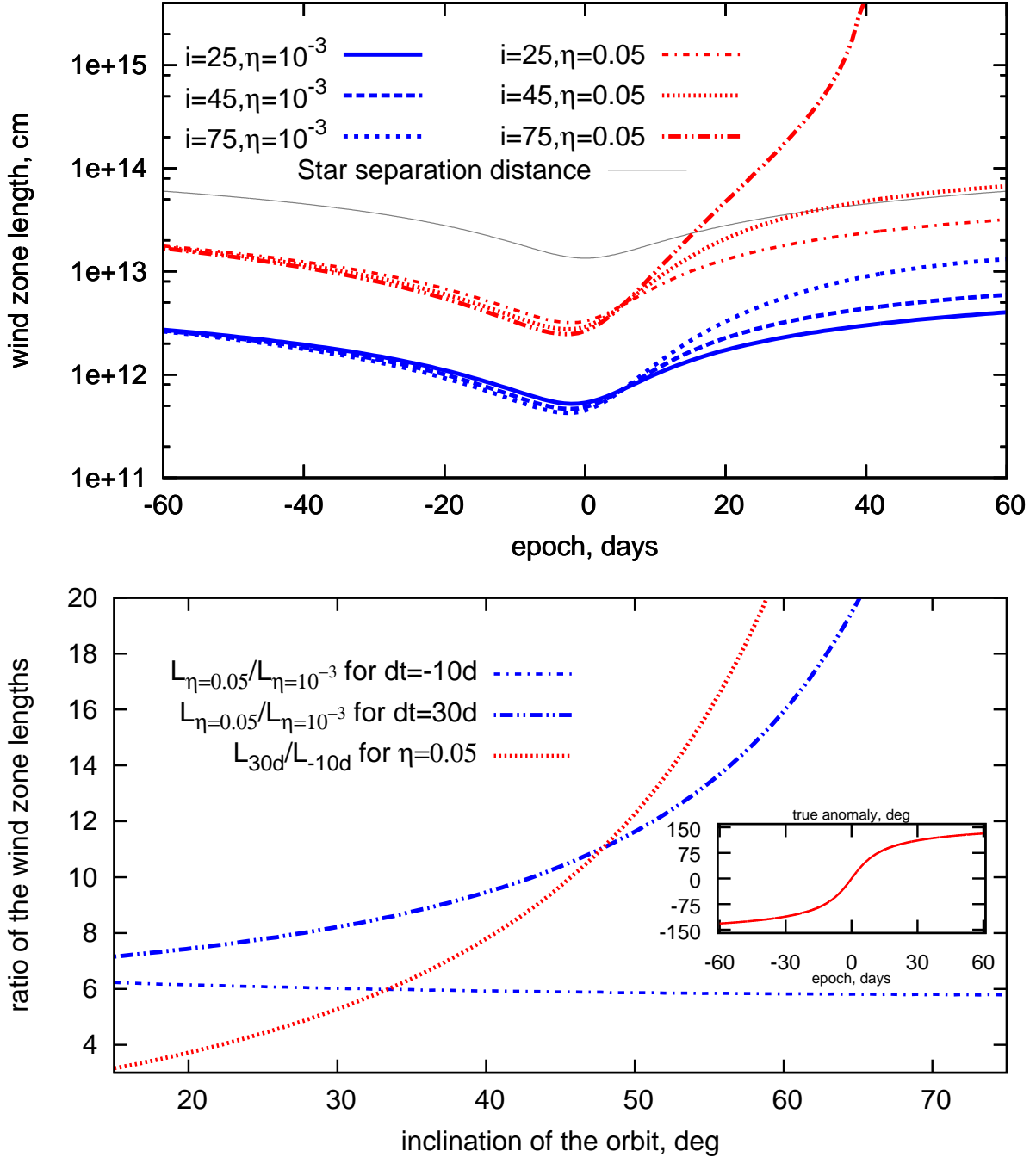


Fig. 1.— Upper panel: PWZ lengths towards the observer as a function of days to periastron. The calculations are performed for two values of the η -parameter: $\eta = 10^{-3}$ (CD) and $\eta = 0.05$ (SW) and three different orbital inclinations: $i = 25^\circ$, $i = 45^\circ$, and $i = 75^\circ$. Bottom panel: ratio of the PWZ lengths for the interaction with SW and CD for -10 d (dot-dashed line) and $+30$ d (dash-dot-dotted line) to periastron passage; and expected ratio of the post- to pre-periastron flares (dotted line). The inset plot shows dependence of the true anomaly (in degrees) on the epoch (in days) to periastron.

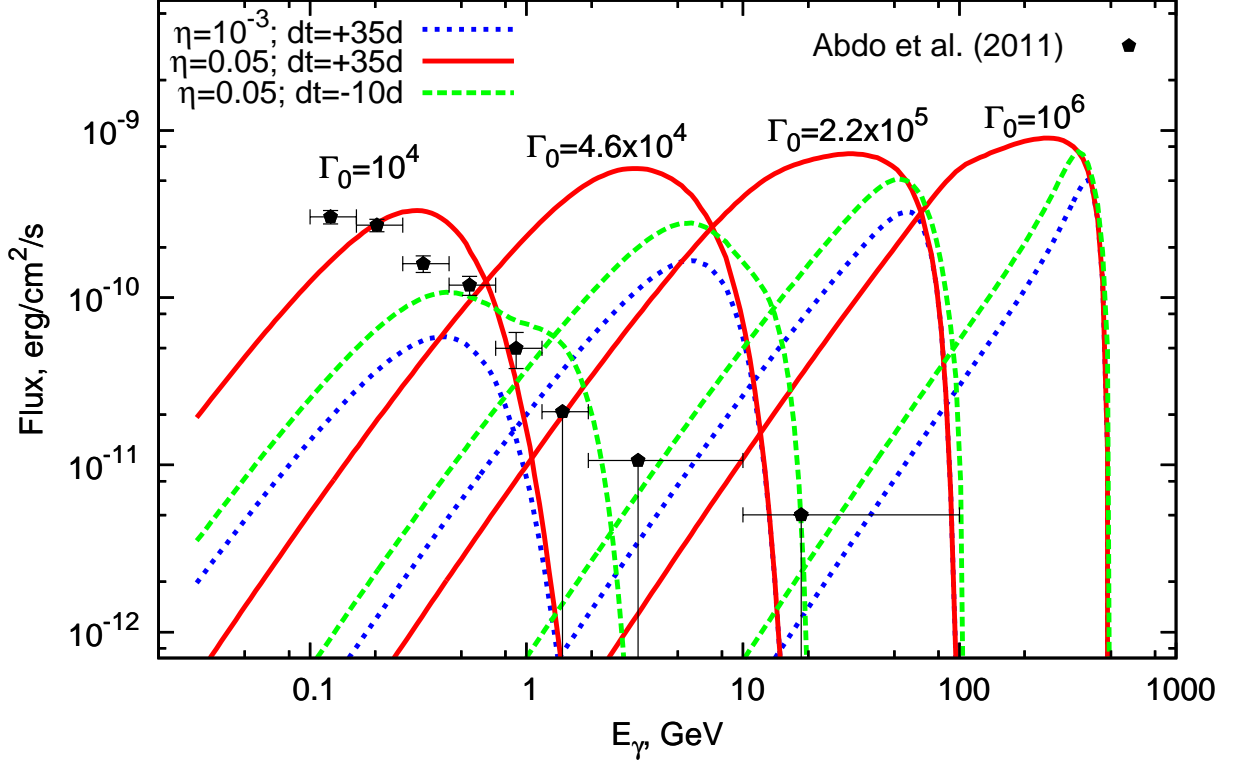


Fig. 2.— The spectral energy distribution of the IC radiation of the unshocked pulsar wind at the epoch of 35 days after periastron passage ($\eta = 10^{-3}$ —dotted lines; and $\eta = 0.05$ —solid lines) and at the epoch of 10 days before periastron passage ($\eta = 0.05$ — dashed lines). The calculations are performed for two target photon fields: (i) radiation of the companion optical star with a radius $R_* = 6.2 \times 10^{11}$ cm and the surface temperature $T_* = 3 \times 10^4$ K, and (ii) radiation of the CD, which was assumed to be isotropic gray body with temperature $T_r = 10^4$ K and energy density $w_{\text{ph}} = 2.8 \text{ erg cm}^{-3}$. Several initial pulsar wind bulk Lorentz factors have been assumed: $\Gamma_0 = 10^4$, 4.6×10^4 , 2.2×10^5 and 10^6 . It is assumed that the kinetic energy luminosity of the cold ultrarelativistic pulsar wind is equal to the SDL of the pulsar. The calculations performed for the model parameters $\eta = 5 \times 10^{-2}$ and $\Gamma_0 = 10^4$ match quite well the observational points (pentagons) reported by the *Fermi* LAT collaboration for the post-periastron flaring episode (Abdo et al. 2011).

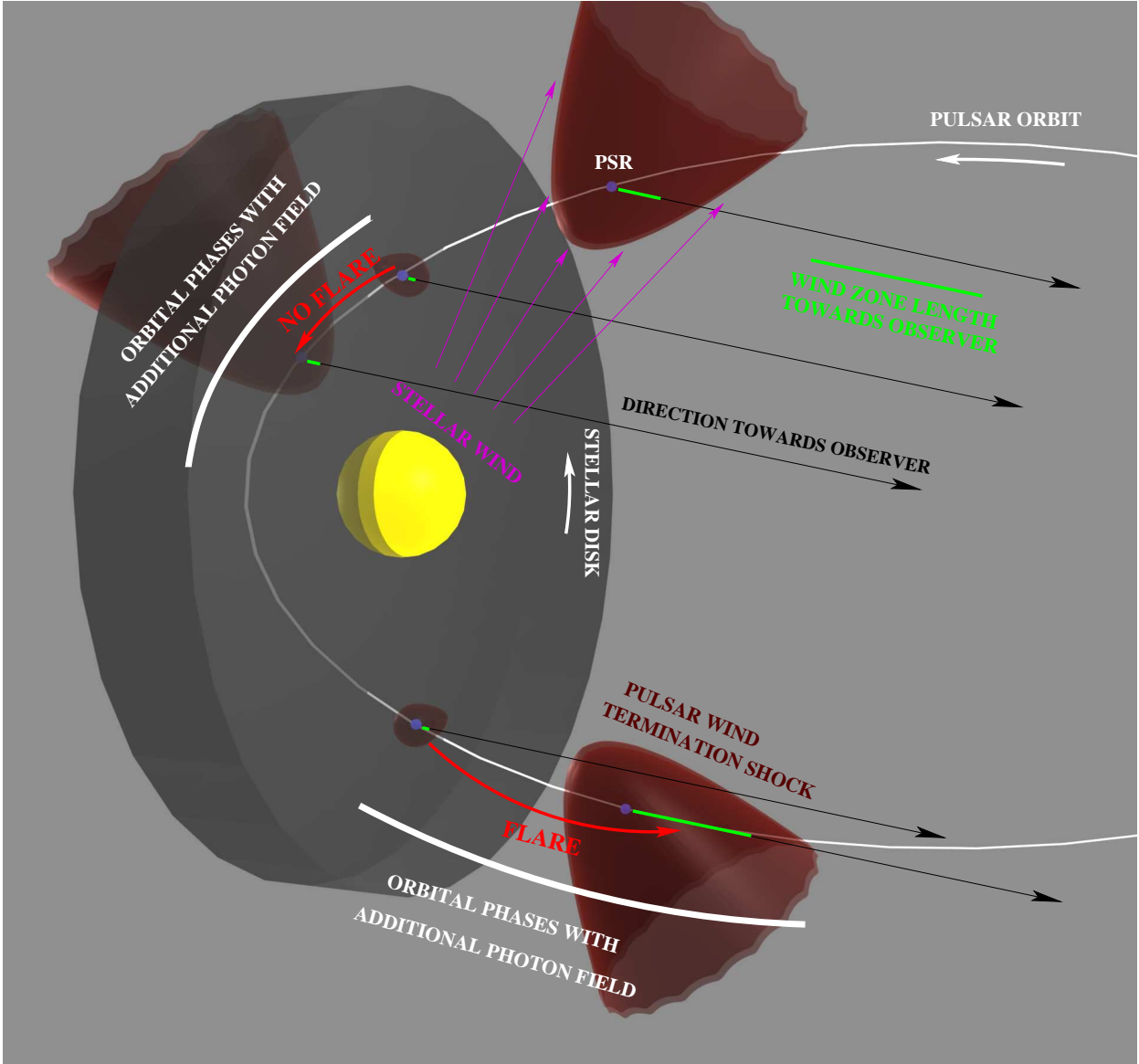


Fig. 3.— Sketch of the scenario.

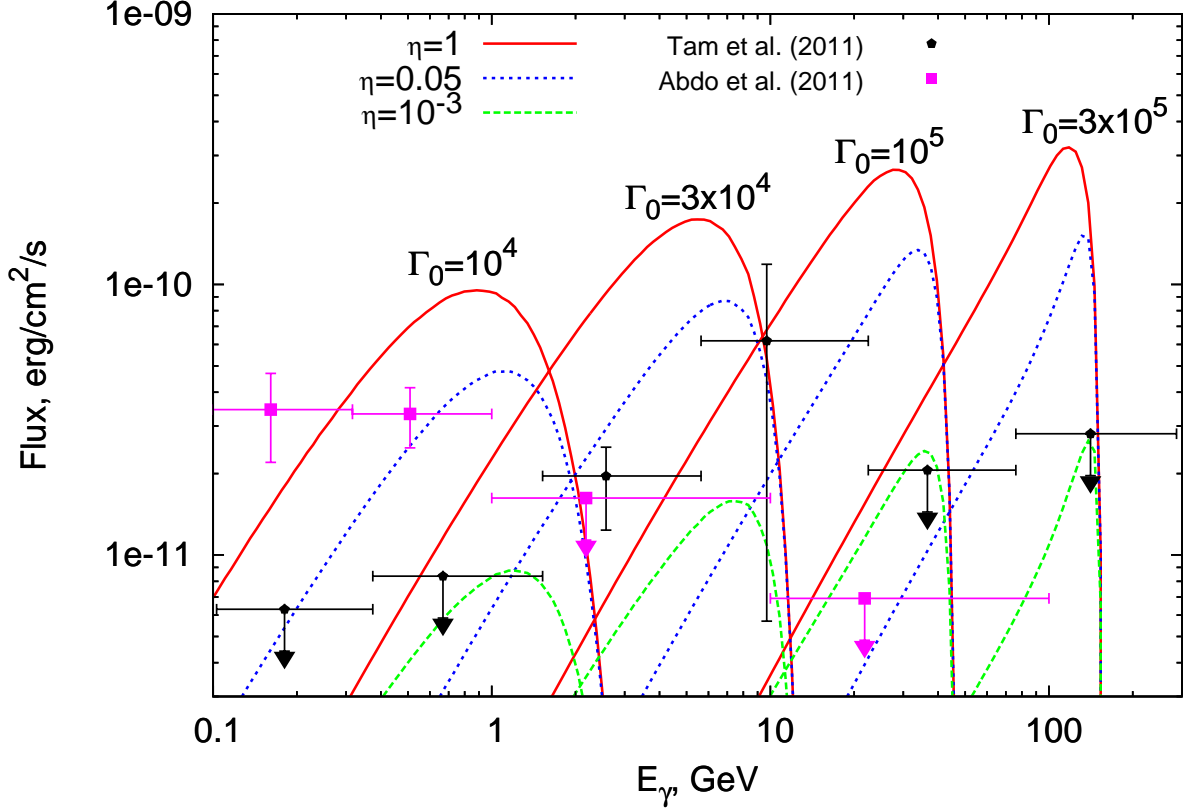


Fig. 4.— Spectral energy distributions of IC radiation of the unshocked pulsar wind averaged over the period from -35 to $+18$ days around the periastron passage. The calculations are performed for different values of the η -parameter: $\eta = 1$ (solid lines), $\eta = 0.05$ (dotted lines, SW) and $\eta = 10^{-3}$ (dashed lines, CD), and the pulsar’s wind bulk Lorentz factor: $\Gamma_0 = 10^4$, 3×10^4 , 10^5 and 3×10^5 . The densities of target photons at different positions of the wind are calculated assuming a spherical star with a radius $R_* = 6.2 \times 10^{11}$ cm and surface temperature $T_* = 3 \times 10^4$ K (see for details Negueruela et al. 2011; Khangulyan et al. 2011). The gamma-ray measurements correspond to the period of $[-35, 0]$ days (pentagons) reported by Tam et al. (2011), and the period of $[-28, 18]$ days (squares) reported by Abdo et al. (2011).